Core effects on the polarization of optical Rydberg transitions following electron capture into slow, highly ionized neon recoil ions

L. J. Lembo,* K. Danzmann, Ch. Stoller,† W. E. Meyerhof, and T. W. Hänsch‡
Department of Physics, Stanford University, Stanford, California 94305-4060
(Received 22 December 1986; revised manuscript received 24 August 1987)

Polarization measurements have been performed and emission spectra in the visible and near ultraviolet have been acquired for transitions between Rydberg states of slow, highly charged neon ions (Ne^{q+}, with $q=10-5$, and $v\approx 0.09$ a.u.), following electron capture from Na. Resolvable line splittings appear in those spectra for which the incoming projectile ions carry L-shell core electrons. The optical emission cross sections are much smaller for these ions and the radiation is significantly depolarized relative to those ions whose transitions are seen as structureless. These effects are attributed to the inhibition of Stark mixing by core interactions.

I. INTRODUCTION

The development of sources, such as the recoil-ion source,[1] of highly charged, low-energy (HQLE) ions has encouraged various investigations into the physics of highly charged systems. Free of the large Doppler, collisional, and high-field effects present in conventional ion sources, the recoil ion source suggests the application of high-resolution spectroscopy to the study of highly charged ions. For this purpose, one can exploit electron-transfer collisions which selectively populate highly excited states of slow ions. Optical studies of these ions would also promote an understanding of the electron capture process itself. A complex quantum-mechanical three-body process, electron capture constitutes a problem of fundamental interest; it may also have practical applications in the development of uv or x-ray lasers and be crucial in understanding the dynamics of astrophysical and fusion plasmas.

This paper summarizes the results of our investigations of the optical spectra emitted by Rydberg states ($n\approx 10$) of highly charged neon recoil ions (Ne^{q+}, with $q=10-5$) after slow electron-capture collisions ($v\approx 0.09$ a.u.) with sodium. Optical spectra, obtained with classical grating spectroscopy, are presented. Partial optical-emission cross sections for the various levels have been obtained. The polarization of the pertinent spontaneous emission has been measured. The data are compared to theoretical predictions and analyzed to yield evidence for the effects of ion core interactions on the electron-capture process. Preliminary results of our efforts have been published previously.[2,3]

II. MOTIVATION

A. Theory

The partial cross sections for capture into the various (n,l,m) substates of the projectile ion play an important role in most studies of highly charged ions. The classical barrier model (CBM) is a simple yet useful model for describing electron transfer.[4,5] It allows a prediction of the principal n quantum number characterizing the states most likely to be populated in collisions involving slow, highly ionized species. More intricate theories are necessary for predicting the distribution of angular-momentum l and magnetic m substates populated by electron transfer.

It is claimed[6] that many approaches to the calculation of the angular-momentum substate distributions fail to take proper account of the Stark mixing of the projectile sublevels by the electric field of the residual (postcapture) target ion. As a result, these theories find that the capture process leaves the angular-momentum sublevels populated by their statistical weights.[7]

In order to treat the problem of Stark mixing, Salin[6] has performed calculations for slow electron-transfer collisions of bare ions on atomic hydrogen using exact (adiabatic) one-electron diatomic molecule (OEDM) states as a basis set. Transitions take place at molecular curve crossings via radial coupling of the molecular states. The initial separated-atom state is an atomic s state, which correlates to a molecular σ state ($m=0$ along the molecular axis); radial coupling will cause transitions to take place only to other σ states. The quantization axis used in these calculations is the internuclear axis; if the collision velocity is small compared to the velocity of the orbiting electron, the molecular orbital will follow the rotation of the internuclear axis. If the σ state in which the electron is initially populated was able to follow the internuclear axis perfectly, the resulting separated-atom state, referred to a quantization axis parallel to the direction of the projectile's motion, will be an atomic state for which the magnetic quantum number m is zero. The finite rate of rotation will give rise to some rotational mixing among the m substates; at the ratio of projectile to electron velocities used in our studies, Salin finds the final magnetic-substate distribution to be left with a high degree of final alignment, with the $m=0,\pm 1$ substates dominantly populated. Thus, slow electron transfer is predicted to populate the l sublevels with a high degree of m-substate alignment, and not statistically. These calculations show that, due to Stark mixing among the l sublevels, the final l,m-substate distribution is character-

ized by equal populations of all l sublevels with a given m value. If $W(l,m)$ is the population of an (l,m) substate, this result may be expressed as

$$W(l,m)=W(m)\ ,$$

independently of l for some function $W(m)$, which Salin calls the "complete-mixing distribution." In this sense, the final magnetic-substate alignment is more representative of the primary capture than is the angular-momentum sublevel distribution, thereby justifying strong experimental efforts to measure the m-substate distribution.

It should be emphasized at this point that these calculations were performed for bare projectile ions, for which the separated-atom l sublevels are degenerate; hence, Stark mixing has a strong influence on the character of the stabilized eigenfunctions. If the incoming projectile ion carries core electrons, the l sublevels are no longer degenerate, the ability of a weak electric field to mix the l sublevels is diminished, and calculations for the final substate distributions must be reconsidered. Hence, it may prove interesting not only to search for some manifestation of the magnetic-substate alignment, but to examine the trend in this effect as the projectile-ion cores become larger.

B. Previous experiments

Several experimental investigations have been concerned with the influence of the core on the l distributions.[8,9] It has been observed that the distributions undergo qualitative changes as the size of the core increases. The velocity dependence of the l distributions has also been investigated in these studies;[10] it has been found that the distributions are strongly velocity dependent, approaching a nearly statistical distribution at high velocities ($v \approx 0.5$ a.u.). Calculations[11] performed for bare projectile ions indicate that as the projectile velocity is decreased this statistical distribution should persist for velocities $\ll 0.1$ a.u. However, measurements at these low velocities performed to date have been possible only for collision systems in which the projectile ion carries core electrons, and usually for capture into levels rather close to the core. In these experimental studies the l distribution has been seen to deviate qualitatively from a statistical one for velocities as high as 0.3 a.u.[8] in agreement with atomic-orbital (AO) calculations by Fritsch and Lin.[12] Using optical spectroscopy, Sorensen *et al.*[13] have even observed nonstatistical populations at much higher velocities ($v=2$ a.u.).

It would therefore appear that, in collision systems for which an l distribution has been reported, interactions of the captured electron with the core are always an important influence at low velocities. Thus far, no cases have been reported for which the core is of little or no importance in determining the final substate distributions.

The investigation of such cases by means of photon spectroscopy requires a much higher resolution, since, as the interaction with the core becomes small, the various l sublevels of the captured electron approach degeneracy. An alternative gauge of the core influence would be helpful in these situations. A complete characterization of the capture process necessitates a specification of the magnetic substate m distribution as well as the l distribution. Deviations from a statistical population of the magnetic m substates manifest themselves as anisotropy or polarization of the emitted radiation. This alignment effect is well known[14] for fast collisions where the projectile has a velocity much larger than the velocity of the target electron in its bound state. For slow collisions the alignment of low-lying p states has been measured by Baptist *et al.*[15] and Vernhet *et al.*[16] Polarized optical emission from Rydberg states has been observed and reported by us in a previous communication[2] for collision systems involving projectiles having $1s$ core electrons. Such polarization effects, indicative of the m-substate population, are easily detected even in cases for which the l sublevels are difficult to resolve.

III. EXPERIMENT

The experimental arrangement is shown in Fig. 1. Charge-state selected Ne^{q+} recoil ions, provided by the Stanford recoil ion source,[17] are used as projectiles. Ions with $q=10-5$ and energies of $500q$ eV are focused onto an atomic Na vapor jet target, produced by an effusive alkali beam oven maintained at a temperature of approximately 400 °C. We used typical recoil ion currents of up to 10 pA for bare neon and up to 300 pA for Ne^{8+} and lower charge states. Photons emerging from the $Ne^{q+}+Na$ interaction region are focused onto the slit of an Instruments S.A. HR 320 normal-incidence grating

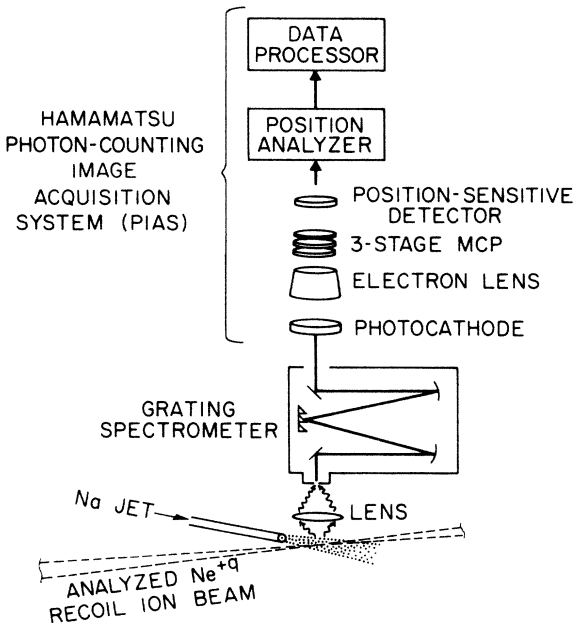

FIG. 1. Experimental arrangement for wavelength measurements. Charge-state selected neon ions are directed onto a Na vapor-jet target. The resulting photons are focused onto the slit of a grating spectrometer. A photon-counting image system positioned in the spectrometer focal plane allows the acquisition of wavelength spectra.

spectrometer with 0.32-m focal length; the photocathode of a Hamamatsu photon-counting image-acquisition system (PIAS) is positioned in the spectrometer focal plane. Two-dimensional images of the focal plane are monitored as they accumulate in real time and are later processed into wavelength spectra. The combination of PIAS spatial resolution, spectrometer focal-plane dispersion, and spectrometer slit width gave a spectral resolution (full width at half maximum) of 50 pm. Acquisition times varied from 20 min to 3 h; the resulting photon counts indicate typical light intensities of 10^2 photons/cm^2 sec incident on the photocathode.

A different optical arrangement, shown in Fig. 2, was employed for the polarization measurements. Interference filters restricted the spectral sensitivity to narrow bands around the lines of interest. A polarization analyzer was added to the optical path; the polarizer could be rotated by 90° into orientations which transmit photons polarized either parallel or perpendicularly to the ion-beam path. These photons were detected with a photon-counting photomultiplier. To eliminate background noise the recoil-ion beam was chopped at a rate of 25 Hz and a lock-in technique was employed. Net count rates were thus determined for both photon polarizations ($I_{\parallel}$ and $I_{\perp}$, respectively), and a degree of polarization P was calculated according to

$$P=(I_{\parallel}-I_{\perp})/(I_{\parallel}+I_{\perp}) . \quad (1)$$

Acquisition times varied from 1 min to 1 h.

IV. RESULTS

A summary of CBM (classical barrier model) predictions, hydrogenlike wavelengths, observed wavelengths, emission cross sections, and polarizations is presented in Table I.

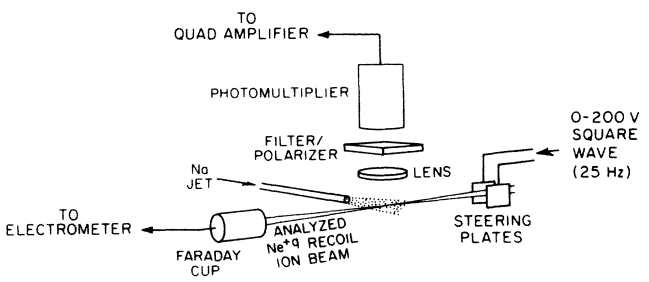

FIG. 2. Experimental arrangement for polarization measurements.

A. Wavelength spectra

Examples of the accumulated spectra are shown in Figs. 3 and 4. All spectra show evidence for photons emitted in transitions following electron capture into states whose principal quantum number is given by the CBM. Using the Hartree-Fock code RCN-RCG,[18] we have calculated the level structure of the systems under investigation. This code includes relativistic corrections and the effects of configuration interaction. The spectral line positions predicted by these calculations are indicated on each of the spectra. The indicated wavelengths are for $\Delta l=-1$ transitions; the $\Delta l=+1$ transitions all have branching ratios smaller than 1% and are negligible. The ion cores are assumed to be in their ground states.

For the $Ne^{9+}+Na$ collision system, the CBM predicts that electron capture will proceed predominantly into $n=10$ states of the heliumlike species Ne^{8+*}. The spectrum for the subsequent $n=10$ to $n=9$ transition is shown in Fig. 3(a). For the $Ne^{8+}+Na$ collision system,

TABLE I. Summary of experimental results for Rydberg transitions after charge exchange collisions: $Ne^{q+}+Na \rightarrow Ne^{(q-1)+*}+Na^{+}$. n_{CBM}, principal quantum number expected from classical barrier model; σ_{opt}, optical emission cross section.

q	n_{CBM}	Transition	H-like λ (nm)	Observed λ (nm)	σ_{opt} (10^{-15} cm^2)	Polarization
10	10.9	$n=10\rightarrow n=9$	388.5	388.5 ±0.15	2.2 ±0.2	0.34±0.08
		$n=9\rightarrow n=8$	277.9	277.9 ±0.15	2.1 ±0.2	
9	10.0	$n=10\rightarrow n=9$	479.62	479.64±0.05	2.0 ±0.1	0.31±0.01
		$n=9\rightarrow n=8$	343.07	343.07±0.07	3.2 ±0.2	0.28±0.02
8	9.1	$n=9\rightarrow n=8$	434.19	434.21±0.06	2.5 ±0.1	0.30±0.01
		$n=8\rightarrow n=7$	297.68	297.68±0.04	2.6 ±0.1	0.26±0.01
7	8.1	$n=8\rightarrow n=7$	388.81	388.53±0.04 386.56±0.06	0.38±0.02	0.23±0.02
6	7.2	$n=7\rightarrow n=6$	343.48	343.76±0.07 342.93±0.07 341.15±0.07	0.54±0.03	0.15±0.01
5	6.2	$n=6\rightarrow n=5$	298.23	297.68±0.08 296.80±0.08 296.28±0.08		0.08±0.01

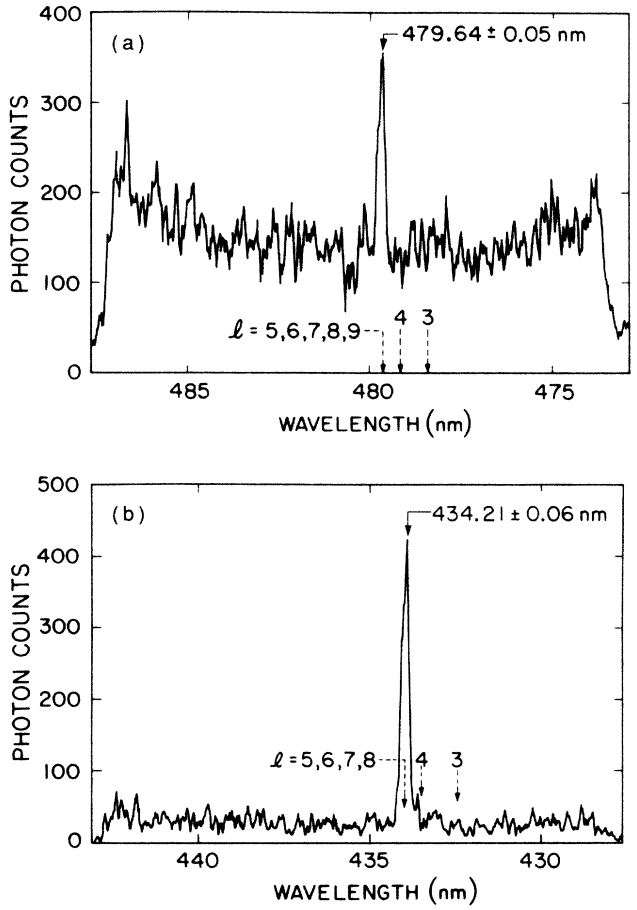

FIG. 3. Spectra for Ne^{8+*} and Ne^{7+*} ions, each showing an unresolved line at the respective hydrogenlike wavelengths. Hartree-Fock predictions for transitions originating at various angular-momentum (l) sublevels are indicated by dashed lines. Ground-state cores are assumed. (a) $n=10$ to 9 transition of Ne^{8+*} following capture by Ne^{9+}. (b) $n=9$ to 8 transition of Ne^{7+*} following capture by Ne^{8+}.

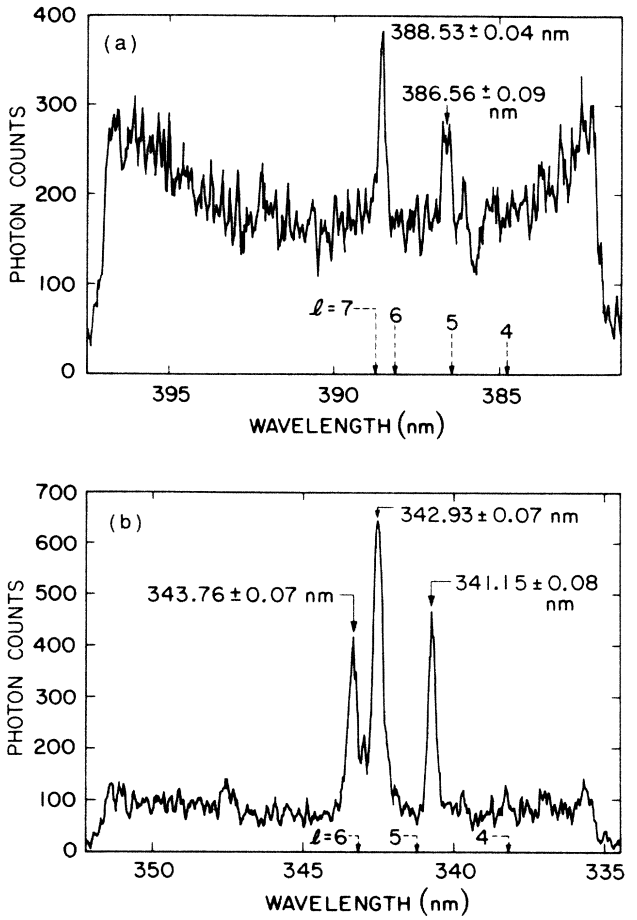

FIG. 4. Spectra for Ne^{6+*} and Ne^{5+*} ions. Hartree-Fock predictions indicated as in Fig. 3. (a) $n=8$ to 7 transition of Ne^{6+*} following capture by Ne^{7+}. (b) $n=7$ to 6 transition of Ne^{5+*} following capture by Ne^{6+}.

the CBM predicts that electron capture will proceed predominantly into the $n=9$ states of the lithiumlike species Ne^{7+*}; the spectrum for the subsequent $n=9$ to $n=8$ transition is shown in Fig. 3(b). Both spectra show single unresolved spectral lines whose wavelengths are equal to the corresponding hydrogenlike values. According to the results of the Hartree-Fock code, photons contributing to the spectral lines in Fig. 3 are emitted in transitions originating in upper states having angular-momentum quantum numbers $l \geq 5$. Since the branching ratios for the decay of states with low l values via $\Delta n = -1$ transitions are known,[19] one can, from the absence of other fine-structure components in Fig. 3, establish upper limits on the population of these low angular-momentum states. In this way, we find that the partial cross sections for capture into s and f states are smaller than the average cross section for population of a high l state, $\sigma_{s,f} < \sigma_{l>5}$. The partial cross sections for capture into p and d states are less than three times the value for a high l state, $\sigma_{p,d} < 3 \cdot \sigma_{l>5}$. These results are compatible with the predictions of Salin's complete l-mixing model.[6]

In contrast to the $Ne^{9+}+Na$ and $Ne^{8+}+Na$ cases, we see several resolved lines in the spectra for transitions following electron capture by projectile ions having L-shell ($n=2$) electrons in their ground-state cores. The $n=8$ to $n=7$ transition following capture by Ne^{7+} has a hydrogenlike wavelength of 388.8 nm; the observed spectrum for this transition is shown in Fig. 4(a). The $n=7$ to $n=6$ transition following capture by Ne^{6+} has a hydrogenlike wavelength of 343.5 nm; the observed spectrum is shown in Fig. 4(b). For the Ne^{6+*}, Ne^{5+*}, and Ne^{4+*} species, the Hartree-Fock calculations indicate that the energy splittings created by interaction with a ground-state core will give rise to resolvable wavelength splittings for transitions from all upper l sublevels. The predicted positions of the transitions between these high angular-momentum Rydberg states do not critically depend on spin-orbit coupling and configuration mixing. The observed structure is probably due to l-sublevel splitting via core interactions, although the predicted and observed splittings agree only qualitatively. Work is in progress to identity the various spectral features of these transitions and to explore the influence of excited core configurations, spectator elec-

trons, and spin-other-orbit coupling on the ionic energy-level structure.

B. Metastable ion cores

The Hartree-Fock calculations indicate that metastable cores would interact with the outer (captured) electron strongly enough to give rise to resolvable fine structure for all l sublevels. The absence of any such structure in the Ne^{7+*} spectrum [Fig. 3(b)] suggests that less than 10% of the ions which emit visible photons possess metastable cores. Recoil-ion sources, on the other hand, are well known to produce large amounts of metastable ions.[20] Because the transit time through our analyzing magnet is 1.5 μs, any metastable recoil ions created in the $(1s2s)^3S$ state, with a lifetime of 70 μs,[21] will survive to reach the interaction region. From x-ray spectra taken with a gas-flow proportional counter, we know that the ratio of K to L x rays is about one to three; this suggests that a large fraction of the recoil ions reaching the sodium target is indeed in metastable states. These ions capture an electron as readily as ground-state ions and the competition between autoionization, x-ray emission, and visible emission determines the major decay path. Using the RCN-RCG code[18] and first-order perturbation theory, we have calculated the relative rates of these decay branches for quartet and doublet states that can exist after capture. For capture into high angular-momentum states (always assuming a triplet core), we found that the radiative $\Delta n = -1$ transitions completely dominate over Auger decay for all terms (doublet and quartet are strongly mixed for these states), typical radiative and Auger decay rates being 10^9 s^{-1} and 10^6 s^{-1}, respectively. A metastable recoil ion capturing an electron into a Rydberg state should thus contribute to our optical spectra, if the core is conserved in the capture process. Core conservation has been demonstrated by Brazuk *et al.*[22] for capture from Li into O^{4+}, N^{3+}, and C^{2+}. In our case, capture takes place at even larger internuclear distances, but we do not see any structure pertinent to excited cores in our optical spectra. We must conclude that most of the metastable cores are destroyed by a spin-flip collision or deexcitation by x-ray emission following mixing of the $2s$ and $2p$ states by collisions in the sodium target. The latter process is known[23] to be the dominant loss mechanism for He^+ metastables in slow collisions with neutral atoms.

C. Optical emission cross sections

The optical emission cross sections for the various observed lines are listed in Table I. The quoted errors refer to the statistical errors of the relative intensities, including small temporal fluctuations of the target density. The absolute scale is probably accurate only to an order of magnitude because it was obtained by normalizing to the density of our target as calculated from the temperature of the Na oven and the measured spatial structure of the Na jet. It is nevertheless instructive to compare these partial emission cross sections to total capture cross sections, measured by the energy-gain

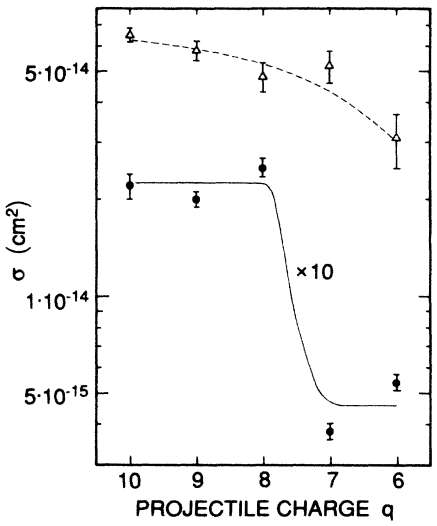

FIG. 5. Partial optical emission cross sections (bold symbols, solid line to guide the eye) and total capture cross sections (light symbols, broken line to guide the eye) vs projectile-ion charge state.

method for similar collision systems.[24] From Fig. 5, it can be seen that the total capture cross section is only a slowly varying function of the initial charge state, whereas the optical emission cross section shows a dramatic decrease for projectiles with $q \leq 7$. These ions have L-shell electrons in their cores and show a large line splitting in our optical spectra. Optical emission is dominated by high angular-momentum states, because these cannot decay by x-ray emission. Low angular-momentum states, which decay preferentially by x-ray emission, have relatively small branching ratios for visible decay branches. Our experiment suggests that electron capture proceeds predominantly into low angular-momentum states if the degeneracy of the final levels is removed. Such a behavior was also suspected by Dijkamp *et al.*[8] for capture into low-n states.

D. Polarization

A summary of our polarization results is given in the last column of Table I. All measured transitions are found to be polarized in varying degrees along the direction of the incident recoil-ion velocity. This clearly indicates that the m-substate distribution is not a statistical one, for which symmetry demands that the emitted radiation be unpolarized ($P = 0$). For the $q = 10$, 9, and 8 projectiles, the first $\Delta n = -1$ transitions subsequent to capture into n_{CBM} are all characterized by polarization degrees which are equal within the experimental errors. Below $q \leq 7$ there is a marked decrease in polarization for decreasing projectile charge state.

The polarization uncertainties cited are one standard deviation photon-counting statistics. In principle, there are other sources of random error which could contribute. These would include fluctuations in the effective Na-target density (or, equivalently, fluctuations in the position of the recoil-ion beam), which take place on a

time scale comparable to the polarizer-switching time, and extraneous photon counts caused by Van de Graaff x-ray bursts ("sparks"). During any given experimental run, measurements of P for each transition were repeated several times; the resulting sample standard deviations were consistent with those listed in table I, implying that photon-counting statistics represent the only significant source of random error.

There are also several possible sources of systematic error for the polarization measurements. One of these is the fringing field of the analyzing magnet for the recoil ions; Hall-probe measurements reveal that this has a strength in the secondary-interaction region of 8 G, in a direction perpendicular to the observation axis and the recoil-ion velocity. Following electron capture, the magnetic-substate distribution will undergo precessional rotation through an angle of 4° during a typical upper-state lifetime of 1 nsec. The situation is equivalent to observing photons emitted at an angle of 86° instead of 90° to the direction of the recoil-ion beam. This would decrease the observed degrees of polarization by less than 1%.

With the present arrangement of ion optics, we must also consider our inability to know the precise direction of the recoil-ion velocity with respect to the optical axis of the polarizer. From the geometry of the magnet exit hole assembly, we can estimate this uncertainty to be ±5°; the result of this would be that the polarizer, instead of analyzing photons polarized parallel and perpendicularly to the ion-beam direction, could be analyzing photons polarized at 0±5° and 90±5°. It is straightforward to show that a dipole field whose true degree of polarization is 0.300 would, in the case of a 5° misalignment of the polarizer axis, have an apparent degree of polarization equal to 0.296. As in the case of magnetic-field precession, this is a small effect in comparison with the photon-counting statistics.

An effect which is somewhat more difficult to treat analytically is the deposition of thin, depolarizing films of sodium or vacuum-pump oil, for example, on the high-vacuum surface of the observation window. Fluctuations in the measurements of P over several runs were consistent with counting statistics on any given day, indicating a negligible influence of this effect.

A more important source of systematic error stems from an unexplained continuum radiation underlying the observed lines emitted after capture by $q=7$, 6, and 5 projectiles, which was too weak to show up in the PIAS spectra. Preliminary analyses have been performed on the continuum background by employing interference filters whose passbands were situated on either side of the transition wavelengths measured from the corresponding PIAS spectra. Polarization measurements showed the photons being transmitted by these filters to be unpolarized. Since the filters used to make the polarization measurements transmit both the discreet and continuum emissions, the unpolarized background will decrease the apparent degree of polarization for the photons being emitted on the transitions of interest. The raw polarization measurements reflect a weighted average over the filter bandpass of the polarizations of the continuum photons and the line-radiation photons. In each case, the effect of the continuum background is to decrease the apparent polarizations by $\approx 10\%$ relative to the actual (line) polarizations. The values of the measured polarization for the transitions following capture by the $q=7$, 6, and 5 projectiles were corrected; these modified values appear in Table I.

V. ANALYSIS OF POLARIZATION

A. Theoretical background

Anisotropy of an excited electronic state is manifested through the polarization and angular distribution of the spontaneous decay radiation. If the excited state decays via dipole-allowed transitions, then these properties of the radiation field can be completely determined by a measurement of four judiciously chosen experimental quantities; one such set of quantities are the Stokes parameters.[25] These are degrees of polarization, which are defined in terms of various observation angles and polarization states; one of these parameters is (conventionally) "the" degree of polarization which is defined in Eq. (1). Apart from an intensity normalization, the measurement of four independent Stokes parameters represents the maximum amount of information obtainable from an analysis of the (dipole) radiation field, and thus obviates the need for angular-distribution measurements.

The characteristics of the radiation field are related to the properties of the source which give rise to it, namely, the post-collision electronic state. The shape of the electronic distribution may be expressed in terms of its multipole moments; the vector and tensor moments are commonly referred to as the orientation vector and alignment tensor, respectively, and are related to certain expectation values of the angular-momentum operator.[25,26] The complete analysis of a dipole radiation field determines four of these multipole components: One orientation and three alignment-tensor components.[26,27]

The simplest type of polarization experiment is one such as ours, in which an unpolarized projectile beam is incident on a gas target and photons are detected without coincident projectile-ion detection. In these cases, cylindrical symmetry about the projectile-velocity direction requires that the post-collision state be representable by an incoherent superposition of m substates. Symmetry considerations also demand that the orientation vector (expectation value of J) vanish and that only one component of the alignment tensor be nonzero, namely, the component which describes alignment along the collision axis.[26] In terms of the radiation field, only one of the Stokes parameters is nonzero—the parameter defined as the degree of polarization in Eq. (1). Thus, in experiments possessing rotational symmetry, the degree of polarization represents the maximum information which an analysis of the radiation field alone can reveal concerning the alignment of a given l sublevel.

In general, of course, the capture process populates a distribution of upper substates. For experiments possessing cylindrical symmetry, the density matrix in the

(j,m_j) representation describing the state of the system after capture must be diagonal in m_j. If the Hamiltonian describing the capture process is independent of spin, then the post-capture state can be fully described by a density matrix in the l,m_l basis, which must be diagonal in m_l immediately after capture. This symmetry argument cannot be extended to rule out the possibility of coherences between upper-state substates of equal m but different l; in fact, experiments performed in fast (≈ 1 MeV/amu) beams have observed such coherences by detecting anisotropic behavior in the system.[28]

Since there is no evidence for any such coherences populated in slow collisions all our polarization calculations were performed under the assumption of complete incoherence of all (l,m) substates. In this case, one can simply sum the photon rates from each of the upper states with weights given by the product of the radiative branching ratios and the rate at which that state is populated by capture.

B. Spin-orbit coupling

For our systems, the spin-orbit splitting is much greater than the natural (radiative) linewidth ($\tau_{so} \ll \tau_{rad}$) and, therefore, might be expected to have a depolarizing effect. The diagonal elements of the density matrix as expressed in the l,m_l basis will become time dependent; this simply represents the precessional variation of the m_l-state populations. More importantly, the density matrix will develop off-diagonal (coherence) elements whose time average is nonzero. These coherences will invalidate the simple method of coherent transition-rate addition in this basis. Calculation of the total emission rates under conditions of spin-orbit depolarization is most conveniently carried out in the total angular-momentum basis (j,m_j).

Using this procedure, the effect of spin-orbit precession was considered. For each of our observed transitions, the expected spin-orbit depolarization is less than the experimental precision in the polarization measurements. This stands in contrast to the situation in experiments which measure the polarization of p to s transitions,[25,26] where spin-orbit coupling reduces the polarization from a value of 1 (complete polarization) to a value of $\frac{3}{7}$. As the l of the upper state increases, the effect of precessional coupling to an angular momentum of $\frac{1}{2}$ (spin) becomes less important. This is illustrated in Fig. 6; polarizations are plotted for l to $l-1$ transitions, assuming that capture exclusively populates the $m=0$ substate of the upper-l sublevel (maximum initial alignment). The solid line shows the polarizations calculated without taking account of spin-orbit effects. The dashed line shows the polarizations calculated with the inclusion of spin-orbit precession. One is led to conclude that, for high-l states, spin-orbit precession has very little depolarizing effect on the radiative emissions. In order for spin-orbit depolarization to be significant, low-l sublevels would have to dominate the radiative emission; for the visible transitions which we observe, just the opposite is the case. It is thus appropriate to discuss our systems in terms of the l,m_l basis.

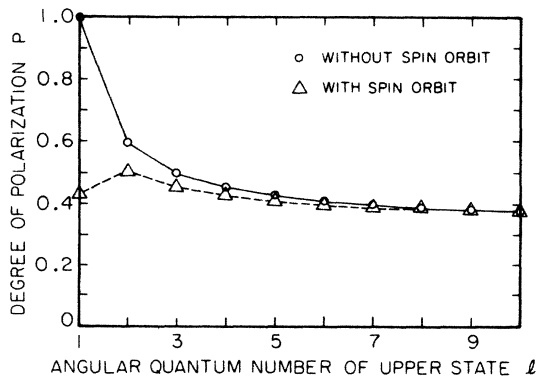

FIG. 6. Polarization of l to $l-1$ transitions, with and without the inclusion of spin-orbit coupling. It is assumed that the population of the (upper) l sublevel resides entirely in the $m=0$ substate.

C. Comparison with theory

In accordance with the discussion of Sec. V A, the degrees of polarization for all (dipole) fine-structure components originating from a given upper-l sublevel, if available, would constitute the most detailed information which the (dipole) radiation field can reveal concerning the m distribution within that l sublevel. Our measurements fall short of this ideal experiment in two ways.

First, our technique for measuring polarizations relies on the use of interference filters of ≈ 10 nm bandwidth; as the spectra in Figs. 3 and 4 indicate, this is insufficient to resolve the various fine-structure transitions. The experimental values for the degrees of polarization pertain to the sum of the fine-structure transitions, weighted by the pertinent transmission coefficients of the interference filter. Since the polarizations of the various fine-structure transitions would not, in general, be identical, the low resolution of the present technique results in a loss of information. In principle, the fine-structure components can be resolved and the degrees of polarization measured for each; this is the subject of ongoing efforts.

The second shortcoming of our measurements is a less fundamental one, and is simply that we have measured degrees of polarization only for $\Delta n = -1$ transitions; this is circumstantial in that the other transitions have wavelengths too far into the ultraviolet to be transmitted by our polarization analyzer. It should be emphasized that when the fine-structure transitions are unresolved, degrees of polarization for these other transitions would yield information which is independent of that contained in the $\Delta n = -1$ polarizations. One should also bear in mind that the quadrupole and higher-order radiative transitions are also sources of independent information, but are extremely weak and would be almost impossible to measure in practice.

At this point, in order to compare with theoretical predictions, we must characterize the entire l,m manifold of substates within a given n shell from knowledge

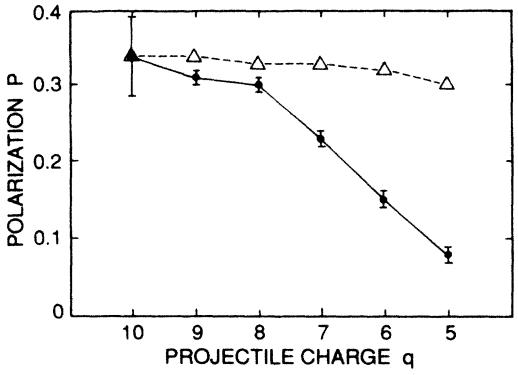

FIG. 7. Polarization of the first $\Delta n = -1$ transition after capture. Solid symbols give our measurements; light symbols give the polarization as calculated from the theoretical m,l distributions of Salin (Ref. 6).

of a single experimental quantity, the polarization. Obviously, we must place some general restrictions upon the form of the distributions, which are consistent with the limits of the l distribution imposed by our PIAS spectra. One such restriction is the complete-mixing assumption of Salin,[6] which characterizes the populations of all l,m substates in terms of the m distribution of the highest-l sublevel. Since calculations for this distribution[6] are given only for the collision system $Ne^{10+}+H$ and capture into the $n=6$ shell, we have to extrapolate the theoretical distribution to higher m values to adapt it to our collision systems. We do this by approximating the Salin distribution by an exponential, which gives an excellent fit. Under these assumptions we generate theoretical l,m distributions for all measured collision systems and calculate the expected degrees of polarization. Complete incoherence is assumed and branching ratios are taken from Lindgard and Nielsen,[19] if available, or assumed to be equal to the hydrogenlike values. A comparison between these theoretical polarizations and our experimental results is shown in Fig. 7. It is obvious that the results for capture from Na by Ne^{q+} projectiles with $q=10$, 9, and 8 are in excellent agreement

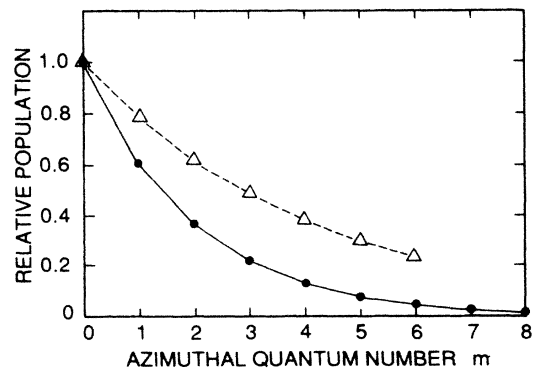

FIG. 8. Exponential m distributions from a fit to our measured polarizations; Ne^{9+} projectiles (solid line), Ne^{6+} projectiles (dashed line).

with the results of a theory pertinent to capture from atomic hydrogen by bare Ne. For $q \leq 7$ the experimental data show a much smaller polarization than would be predicted by this theory; the (exponential) m distribution needed to explain the observed polarization in these cases is much wider than the Salin distribution. Examples of m distributions for $q=9$ and $q=6$ are shown in Fig. 8.

D. Core interactions

The abrupt decrease in polarization starting with the $q=7$ charge state is accompanied by the onset of readily resolvable line splittings in the spectra of the corresponding transitions, and by an abrupt decrease in the partial emission cross sections (see Figs. 3, 4, and 5). These coincidences strongly suggest that the final l,m-substate distributions are being influenced by the interaction of the captured, outer electron with the core electrons. This could come about if intrashell Stark mixing becomes inhibited as the degeneracy of the l sublevels is lifted. Quantitatively, this will occur for Ne ions in which the fine-structure energy splittings have a magnitude which is comparable to or greater than the Stark splitting created by the electric field of the (post-capture) Na^+ ion.

The classical barrier model gives a prediction for the internuclear separation R_x at which primary capture takes place. Some feeling for the importance of the Stark effect on electron capture into Ne^{q+} may be obtained by calculating the first-order Stark splitting induced in the manifold of n_{CBM} states by the electric field of the residual Na^+ ion at a distance equal to R_x. Figure 9 displays, for each charge state, the ratio of first-order Stark splitting to fine-structure (FS) splitting. Here, Δ_{Stark} is the energy difference between the highest- and lowest-energy Stark states in the n_{CBM} manifold (at R_x), and Δ_{FS} is the energy difference between the $l=0$ and highest-l sublevels in the n_{CBM} shell of the unper-

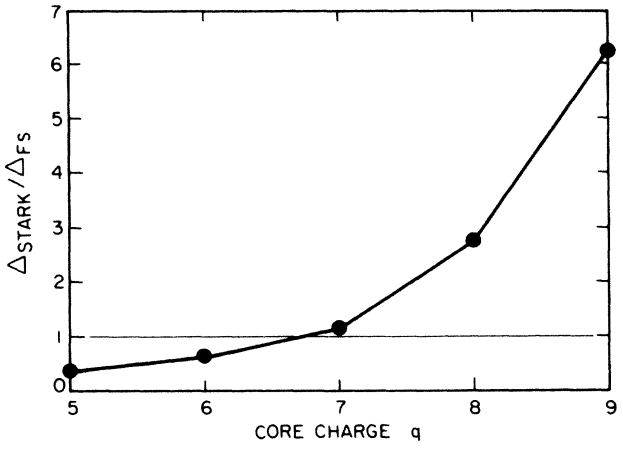

FIG. 9. Ratio of Stark splitting Δ_{Stark} to fine-structure splitting Δ_{FS} at an internuclear distance equal to the crossing radius according to the CBM; as a function of core charge, for capture in collisions $Ne^{q+}+Na$.

turbed $Ne^{(q-1)+}$ ion. For the $q=9$ and 8 projectiles, fine-structure splitting is small in comparison with Stark splitting, and so one might expect the behavior of these ions to be hydrogenlike; hence, the similarity of their polarizations to that of the $q=10$ projectile. On the other hand, fine-structure splitting becomes comparable to Stark splitting for the $q=7$, and dominates for the $q=6$ and 5 projectiles; therefore, we might expect a different physical process, namely the interaction with core electrons, to play a role in determining the electron-capture distributions in these systems.

The precise mechanism by which the suppression of Stark mixing would give rise specifically to decreased partial emission cross sections and polarization degrees is, at this point, a matter for speculation. One explanation is suggested by the electron-capture model of Abramov;[11] this theory predicts that the primary capture process will populate a single Stark state with readily ascertainable quantum numbers.[29] This Stark state may be resolved into its component spherical (nlm) states; the result is that, in addition to exclusively populating the $m=0$ substates, the primary process also favors the lower-l sublevels.

If this be the case, then, when effective, post-collisional Stark mixing will serve to increase the populations in the higher-l sublevels, and transfigure the l distribution to one of the complete-mixing form. On the other hand, when core interactions are strong enough to inhibit Stark mixing, the low-l sublevels will continue to dominate the final substate distribution, invalidating the complete-mixing model. As noted in Sec. IV C, the low-l sublevels radiate weakly in the visible transitions, resulting in the decrease in partial emission cross sections for the $q \leq 7$ projectiles shown in Fig. 5. Other experimental investigations have studied systems where the core influence is stronger than in our studies; their results confirm that low-velocity collisions lead to dominant population of p $(l=1)$ and/or d $(l=2)$ states.[8]

The polarization for the visible transitions $(\Delta n=-1)$ will depend most critically upon the final m distribution in the high-l sublevels. Any process which increases the populations of the low-m states in these high-l sublevels will yield an increase in P. The primary capture process populates only $m=0$ states, but the final l,m distribution will depend upon the relative importance of rotational and Stark mixing. If these are of comparable magnitude, the effect of Stark mixing would be to increase the alignment of the high-l levels by transferring low-m population from low-l to higher-l sublevels. Suppression of this population transfer would decrease the polarization of the visible emissions.

A fundamental problem with the foregoing arguments is that they are essentially heuristic, relying on a description in terms of the separated-atom l,m basis. In fact, we know that the appropriate basis for a bare-projectile plus H-target system is the one-electron diatomic-molecule (OEDM) basis, which, at large distances, closely resembles a Stark basis. In such a basis, the effects of Stark mixing in the adiabatic system have already been accounted for by its very construction; the effects of Stark mixing on the collision process now enter through phase differences among the states. Even a qualitative treatment of this problem should take into account the effect of rotational and radial coupling in the OEDM basis, and not the separated-atom basis. Also, the appropriate adiabatic basis is modified by the addition of core electrons to the projectile ion. For such a collision system, the properties of the state(s) populated by the primary process could be very different than those populated in the hydrogenic-target plus bare-ion systems. This is a difficult theoretical problem and will not be addressed further.

E. Cascading contribution

An intriguing feature of the polarization measurements is that the second $\Delta n=-1$ transitions following capture by the Ne^{9+} and Ne^{8+} projectiles are less strongly polarized than the corresponding first $\Delta n=-1$ transitions. It is tempting to ascribe this to the notion that, in the process of cascading, the m distribution might broaden, resulting in a smaller polarization for the subsequent transition, but closer scrutiny reveals that this is not the case. The polarizations of a single l to $l-1$ transition and of the subsequent $l-1$ to $l-2$ transition due to cascading are found to be identical for any initial m-substate distribution in the upper-l sublevel. This comes about because the tendency of the m-substate distribution to broaden is offset by the tendency of well-aligned l sublevels to result in higher degrees of polarization as l decreases. In the more general case, radiative emission originates from a manifold of l,m substates in some n shell; in such cases, the degrees of polarization for the n to $n-1$ and subsequent $n-1$ to $n-2$ transition due to cascading differ somewhat, but by less than our experimental uncertainty. The inclusion of spin-orbit effects into these cascade calculations does not alter this conclusion.

The depolarization of the second transition must have its origin in a depolarized contribution due to direct capture into the corresponding levels. Although slow electron transfer is selective, the capture process will directly populate the $n_{\mathrm{CBM}}-1$ level to some extent. From the l-sublevel distributions implicit in the complete-mixing m distributions, the values of the radiative branching ratios for all l sublevels involved, and the values of the relative emission cross sections given in Table I, one finds that, for the Ne^{9+} projectiles

$$\sigma_{\mathrm{capture}}(n=9)/\sigma_{\mathrm{capture}}(n=10)=0.94\pm0.10 .$$

For the Ne^{8+} projectiles, one finds, under the same set of assumptions,

$$\sigma_{\mathrm{capture}}(n=8)/\sigma_{\mathrm{capture}}(n=9)=0.38\pm0.06 .$$

Hence, one sees that there is appreciable direct capture into lower n levels.

Rotational mixing is stronger for lower levels because the crossing radius for capture into these levels is small-

er, and, accordingly, the rate of internuclear axis rotation will be higher. One would thus expect the magnetic-substate distributions to be broader for the lower n levels, which would lead to a smaller polarization. The matrix element for rotational ($\Delta m = \pm 1$) transitions is proportional to the rate of internuclear axis rotation $\dot{\Theta}$ so that the transition rate among the m substates is proportional to $\dot{\Theta}^2$. The value of this quantity changes during the collision, and the rotational matrix element also involves angular-momentum expectation values between states which are time and system dependent. Some feeling for the relative importance of rotational mixing for the observed transitions can be gained, however, from estimates for the corresponding values of $\dot{\Theta}^2$. A representative value of $\dot{\Theta}$ may be obtained from the simple expression $\dot{\Theta} = v/R_x$, where v is the velocity of the incoming projectile ion and R_x is the capture crossing radius. In the case of Ne^{9+} and Ne^{8+} projectiles, the values of $\dot{\Theta}^2$ for the lower n level are greater by about a factor of 2 than those for the higher n level, possibly explaining the decrease in polarization. Also noteworthy is the fact that, with the exception of Ne^{10+}, the values of $\dot{\Theta}^2$ for the first transitions following capture are very similar; hence, we can probably rule out rotational mixing as an explanation for the decrease in P for lower charge states.

The smaller degrees of polarization observed on the lower-n transitions after capture by Ne^{9+} and Ne^{8+} ions might also be explained in terms of the influence of core-electron interactions. The l-sublevel splittings (core interactions) will be larger for shells of lower n; however, for the systems we are discussing, the differences in the core interaction from one n shell to the next in an ion of a given charge state are not as dramatic as those created by the addition of L-shell core electrons. Hence, the effect of core interactions on the observed "cascade" depolarization is not amenable to the semiquantitative argument represented in Fig. 9. The extent of depolarization for these cases will depend upon detailed theoretical calculations for an explanation.

VI. CONCLUSION

In conclusion, we have obtained 50-pm FWHM (full width at half maximum) resolution optical wavelength spectra for visible and near uv transitions following electron capture from Na into high-lying n states of slow, highly ionized Ne produced in a recoil-ion source. For ions having only K-shell electrons in their ground-state cores, no resolvable line splitting is seen in the spectra, large optical emission cross sections are obtained, and the polarization of the emitted radiation is in agreement with calculations for one-electron systems. If the incoming ions carry L-shell electrons in their cores, the fine-structure splitting is larger than the Stark splitting induced by the residual target ion, thus inhibiting first-order Stark mixing of low-l and high-l states. In these cases much smaller optical emission cross sections are measured and the emitted radiation is clearly depolarized. This supports the view that a fully successful description of electron capture must take proper account of Stark mixing, and that the complexities of nonsimple cores of the capturing ions are not fully understood. In the future, we will extend our wavelength coverage and spectral integration times, and improve our spectral resolution, in order to see more fine-structure components in the transitions. Thus, we expect to gain some knowledge of the l distribution of capture and, via polarization measurements, of the m distribution within each l sublevel, possibly at various collision velocities. It is also hoped that the spectra reported here will lead to future studies of such Rydberg transitions by high-resolution laser spectroscopy.

ACKNOWLEDGMENTS

We are grateful to R. Gerson for his help with the operation of the PIAS system and to E. Dillard for his technical assistance. This work was supported in part by the National Science Foundation under Grant Nos. PHY8313676, PHY8308271, and PHY8614650.

*Present address: SRI International, 333 Ravenswood Avenue, Menlo Park, CA 94025.

†Present address: Schlumberger Well Services, 5000 Gulf, Houston, TX 77001.

‡Present address: Sektion Physik, Universität of München, D-8000 München 2, Germany and Max-Planck-Institut für Quantenoptik, D-8046 Garching bei München, West Germany.

[1]C. L. Cocke, Phys. Rev. A **20**, 749 (1979).

[2]L. J. Lembo, K. Danzmann, Ch. Stoller, W. E. Meyerhof, and T. W. Hansch, Phys. Rev. Lett. **55**, 1874 (1985).

[3]L. J. Lembo, Ch. Stoller, K. Danzmann, W. E. Meyerhof, T. W. Hansch, and R. Gerson, Nucl. Instrum. Methods B **23**, 101 (1987).

[4]S. B. Elston *et al.* Phys. Lett. **61A**, 107 (1977); H. Ryufuku, K. Sasaki, and T. Watanabe, Phys. Rev. A **21**, 745 (1980).

[5]H. F. Beyer, R. Mann, and F. Folkmann, J. Phys. B **15**, 1083 (1982).

[6]A. Salin, J. Phys. (Paris) **45**, 671 (1984).

[7]R. K. Janev, Phys. Scr. **T3**, 208 (1982).

[8]D. Dijkamp, D. Ciric, and F. J. deHeer, in *Electronic and Atomic Collisions,* edited by D. C. Lorents, W. E. Meyerhof, and J. R. Peterson (North-Holland, Amsterdam, 1986), p. 445.

[9]Yu. S. Gordeev, D. Dijkamp, A. G. Drentje, and F. J. deHeer, Phys. Rev. Lett. **50**, 1842 (1983).

[10]A. Brazuk, H. Winter, D. Dijkamp, F. J. deHeer, and A. Drentje, Nucl. Instrum. Methods B **9**, 442 (1985).

[11]V. A. Abramov, F. F. Baryshnikov, and V. S. Lisitsa, Pis'ma Zh. Eksp. Teor. Fiz. **27**, 494 (1978) [JETP Lett. **27**, 464 (1978)].

[12]W. Fritsch and C. D. Lin, J. Phys. B **17**, 3271 (1984).

[13]J. Sorensen, L. H. Andersen, P. Hvelplund, H. Knudsen, L. Liljeby, and E. H. Nielsen, J. Phys. B **17**, 4743 (1984).

[14]L. D. Ellsworth, B. L. Doyle, U. Schiebel, and J. R. Macdonald, Phys. Rev. A **19**, 943 (1979).

[15]R. Baptist, J. J. Bonnet, G. Chauvet, J. P. Desclaux, S. Dousson, and D. Hitz, J. Phys. B **17**, L417 (1984).
[16]D. Vernhet, A. Chetioui, K. Wohrer, J. P. Rozet, P. Piquemal, D. Hitz, S. Dousson, A. Salin, and C. Stephan, Phys. Rev. A **32**, 1256 (1985).
[17]Ch. Stoller, L. J. Lembo, K. Danzmann, and W. E. Meyerhof, *Abstracts of the Fourteenth International Conference on the Physics of Electronic and Atomic Collisions, Palo Alto, 1985,* edited by M. J. Coggiola, D. L. Huestis, and R. P. Saxon (ICPEAC, Palo Alto, 1985).
[18]R. D. Cowan, *The Theory of Atomic Structure and Spectra* (University of California Press, Berkeley, 1981).
[19]A. Lindgard and S. E. Nielsen, At. Data Nucl. Data Tables **19**, 533 (1977).
[20]E. Justiniano, C. L. Cocke, T. J. Gray, R. DuBois, C. Can, W. Waggoner, R. Schuch, H. Schmidt-Bocking, and H. Ingwersen, Phys. Rev. A **29**, 1088 (1984).
[21]R. Marrus and P. J. Mohr, Adv. At. Mol. Phys. **14**, 181 (1978).
[22]A. Brazuk, D. Dijkamp, A. G. Drentje, F. J. deHeer, and H. Winter, J. Phys. B **17**, 2489 (1984).
[23]M. H. Prior and E. C. Wang, Phys. Rev. A **9**, 2383 (1974).
[24]W. Waggoner, C. L. Cocke, S. L. Varghese, and M. Stockli, Phys. Rev. A **29**, 2457 (1984).
[25]N. Anderson, T. Anderson, J. O. Ostgard Olsen, and E. Horsdal Pederson, J. Phys. B **13**, 2421 (1980).
[26]U. Fano and J. H. Macek, Rev. Mod. Phys. **45**, 553 (1973).
[27]N. Andersen, J. W. Gallagher, and I. V. Hertel, in *Electronic and Atomic Collisions,* edited by D. C. Lorents, W. E. Meyerhof, and J. R. Peterson, (North-Holland, Amsterdam, 1986), p. 57.
[28]K. Ishii, Japan Atomic Energy Research Institute Report No. 85-125, 1985 (unpublished).
[29]B. H. Bransden and R. K. Janev, Adv. At. Mol. Phys. **19**, 1 (1983).